Magnetohydrodynamic Modeling of Shattered Pellet Injection and Impurity Dynamics

by

Brendan C. Lyons[1],

N.M. Ferraro[2], S.C. Jardin[2], C.C. Kim[3], J. McClenaghan[1], L.L. Lao[1], R.M. Sweeney[4], N. Hawkes[5], G. Szepesi[5], J. Kim[6], S. Lee[7], M. Lehnen[8], and JET[9] & KSTAR Contributors

[1] General Atomics
[2] Princeton Plasma Physics Laboratory
[3] SLS2 Consulting
[4]Massachusetts Institute of Technology
[5] Culham Centre for Fusion Energy
[6]Korea Institute of Fusion Energy
[7]Seoul National University
[8]ITER Organization
[9]J. Mailloux, Nucl. Fusion (2022) https://doi.org/10.1088/1741-4326/ac47b4

Presented at the

64th Annual Meeting of the APS Division of Plasma Physics
Spokane, Washington, USA
October 17th, 2022

Modeling of Disruption Dynamics and Mitigation Requires a Multiphysics Model

- **Disruptions pose a risk of damage to future tokamaks, necessitating robust mitigation techniques**
- **Most promising method uses pellet injection of impurities to radiate stored energy**
- **Simulations, validated against mitigation experiments, are required to project techniques to future devices**
- **Integrated model is required to capture all relevant physics**
  - Magnetohydrodynamics (MHD) for macroscopic evolution of disruption dynamics
  - Atomic physics for ionization and radiation from injected impurities
  - Drift-kinetics for phase-space evolution of runaway electron population

M3D-C1 Code Overview

M3D-C1* Solves the Extended-MHD Equations

- **Three-dimensional toroidal geometry**
- **Full (not reduced) MHD**
- **Solves for potential and stream-function fields for $\vec{A}$ & $\vec{v}$ ($\nabla \cdot \vec{B} = 0$ intrinsically)**
- **Includes resistivity, density diffusivity, viscosity, & thermal conductivity**
- **Two-fluid effects (optional)**
- **3D high-order finite elements**
  - Unstructured, triangular mesh in poloidal plane
  - Structured toroidally, but can pack planes
- **Can solve with finite-thickness resistive wall in domain****

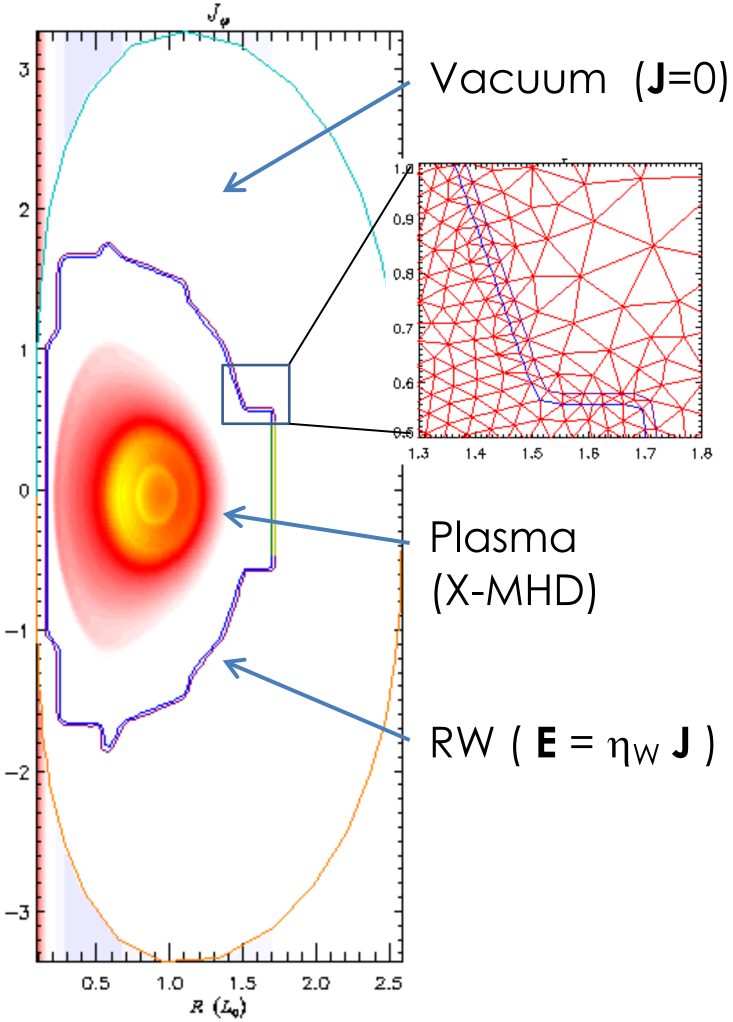

Vacuum (**J**=0)

Plasma (X-MHD)

RW (**E** = η_W **J**)

*S. C. Jardin, et al., Comput. Sci. Discovery 5, 014002 (2012).
**N.M. Ferraro, et al. ,Phys Plasma23 056114 (2016).

M3D-C1 Solves the Extended-MHD Equations

Blue terms are 2-fluid

$$\frac{\partial n}{\partial t} + \nabla \bullet (n\mathbf{V}) = \nabla \bullet D_n \nabla n + S_n$$

$$\frac{\partial \mathbf{A}}{\partial t} = -\mathbf{E} - \nabla\Phi, \quad \mathbf{B} = \nabla\times\mathbf{A}, \quad \mathbf{J} = \nabla\times\mathbf{B}, \quad \nabla_\perp \bullet \frac{1}{R^2}\nabla\Phi = -\nabla_\perp \bullet \frac{1}{R^2}\mathbf{E}$$

$$nM_i\left(\frac{\partial\mathbf{V}}{\partial t} + \mathbf{V}\bullet\nabla\mathbf{V}\right) + \nabla p = \mathbf{J}\times\mathbf{B} - \nabla\bullet\mathbf{\Pi}_i + \mathbf{S}_m$$

$$\mathbf{E} + \mathbf{V}\times\mathbf{B} = \frac{1}{ne}\left(\mathbf{R}_\mathbf{c} + \mathbf{J}\times\mathbf{B} - \nabla p_e - \nabla\bullet\mathbf{\Pi}_e\right) - \frac{m_e}{e}\left(\frac{\partial\mathbf{V}_e}{\partial t} + \mathbf{V}_e\bullet\nabla\mathbf{V}_e\right) + \mathbf{S}_{CD}$$

$$\frac{3}{2}\left[\frac{\partial p_e}{\partial t} + \nabla\bullet\left(p_e\mathbf{V}\right)\right] = -p_e\nabla\bullet\mathbf{V} + \frac{\mathbf{J}}{ne}\bullet\left[\frac{3}{2}\nabla p_e - \frac{5}{2}\frac{p_e}{n}\nabla n + \mathbf{R}_c\right] + \nabla\left(\frac{\mathbf{J}}{ne}\right):\mathbf{\Pi}_e - \nabla\bullet\mathbf{q}_e + Q_\Delta + S_{eE}$$

$$\frac{3}{2}\left[\frac{\partial p_i}{\partial t} + \nabla\bullet\left(p_i\mathbf{V}\right)\right] = -p_i\nabla\bullet\mathbf{V} - \mathbf{\Pi}_i:\nabla\mathbf{V} - \nabla\bullet\mathbf{q}_i - Q_\Delta + S_{iE}$$

$$\mathbf{V}_e = \mathbf{V}_i - \mathbf{J}/ne$$

$$\mathbf{R}_c = \eta ne\mathbf{J}, \qquad \mathbf{\Pi}_i = -\mu\left[\nabla\mathbf{V} + \nabla\mathbf{V}^\dagger\right] - 2(\mu_c - \mu)(\nabla\bullet\mathbf{V})\mathbf{I} + \mathbf{\Pi}_i^{GV}$$

$$\mathbf{q}_{e,i} = -\kappa_{e,i}\nabla T_{e,i} - \kappa_\parallel\nabla_\parallel T_{e,i}$$

$$\mathbf{\Pi}_e = (\mathbf{B}/B^2)\nabla\bullet\left[\lambda_h\nabla\left(\mathbf{J}\bullet\mathbf{B}/B^2\right)\right], \qquad Q_\Delta = 3m_e(p_i - p_e)/\left(M_i\tau_e\right)$$

KPRAD* Provides Needed Atomic Physics Information

- **KPRAD solves for impurity-plasma interaction in low-density, coronal model**
  - N.B. *not* coronal equilibrium
  - Based on ADPAK rate coefficients
  - Impurity charge states and electron density evolve according to ionization and recombination

$$\frac{\partial n_z}{\partial t} + \nabla \cdot (n_z \mathbf{v}) = \nabla \cdot (D \nabla n_z) + \mathcal{I}_{z-1} n_{z-1} - (\mathcal{I}_z + \mathcal{R}_z)\, n_z + \mathcal{R}_{z+1} n_{z+1} + \mathcal{S}_z$$

  - Thermal energy lost from plasma due to
    - Ionization
    - Line radiation
    - Bremsstrahlung radiation
    - Recombination radiation
- **Subcycled much faster than typical MHD time steps**

***D.G. Whyte, et al., Proc. of the 24th Euro. Conf. on Controlled Fusion and Plasma Physics, Berchtesgaden, Germany, 1997, Vol. 21A, p. 1137.**

KPRAD Couples* to the M3D-C1 Temperature Equation(s)

- **Two temperature equations (electron & all-ions)**
  - Dilution cooling of ions and electrons
  - Electrons lose energy to ionization and radiation
  - Main ions cool on electrons

$$n_e\left[\frac{\partial T_e}{\partial t} + \mathbf{v}\cdot\nabla T_e + (\Gamma-1)\,T_e\nabla\cdot\mathbf{v}\right] + \sigma_e T_e = (\Gamma-1)\left[\eta J^2 - \nabla\cdot\mathbf{q}_e - \mathcal{P}_{rad} + Q_{ei} - \Pi_e : \nabla\mathbf{v}\right]$$

$$n_*\left[\frac{\partial T_i}{\partial t} + \mathbf{v}\cdot\nabla T_i + (\Gamma-1)\,T_i\nabla\cdot\mathbf{v}\right] + \sigma_* T_i = (\Gamma-1)\left[-\nabla\cdot\mathbf{q}_* - Q_{ei} - \Pi_* : \nabla\mathbf{v} + \frac{1}{2}\varpi_* v^2\right]$$

- **Single temperature equation**
  - Evolves sum over all species
  - T_e/T_i constant throughout time, implicitly assuming
    - Instantaneous thermal equilibration
    - Split of losses between species evolves as pressure ratio changes

***N.M. Ferraro et al. Nucl. Fusion 59 016001 (2019).**

Verification Benchmarks of NIMROD & M3D-C1

Axisymmetric Benchmark Successful for Fast Impurity Injection in DIII-D Core

- **Four cases solved by both M3D-C1 and NIMROD***
  - Lyons et al., PPCF 61, 064001 (2019)
  - Shown here: argon with Spitzer resistivity
- **Simulation setup**
  - DIII-D shot 137611 @ 1950 ms
  - 2D, nonlinear, single-fluid
  - Fixed boundary
- **Continuous neutral impurity deposition**
  - No impurities to start
  - Gaussian source

$$\frac{dn_z}{dt} = \nu \frac{R_0}{R} \exp\left[-\frac{(R-R_0)^2 + (Z-Z_0)^2}{2\delta^2}\right]$$

  - Injection rate ~1 mm Ne/Ar per ms

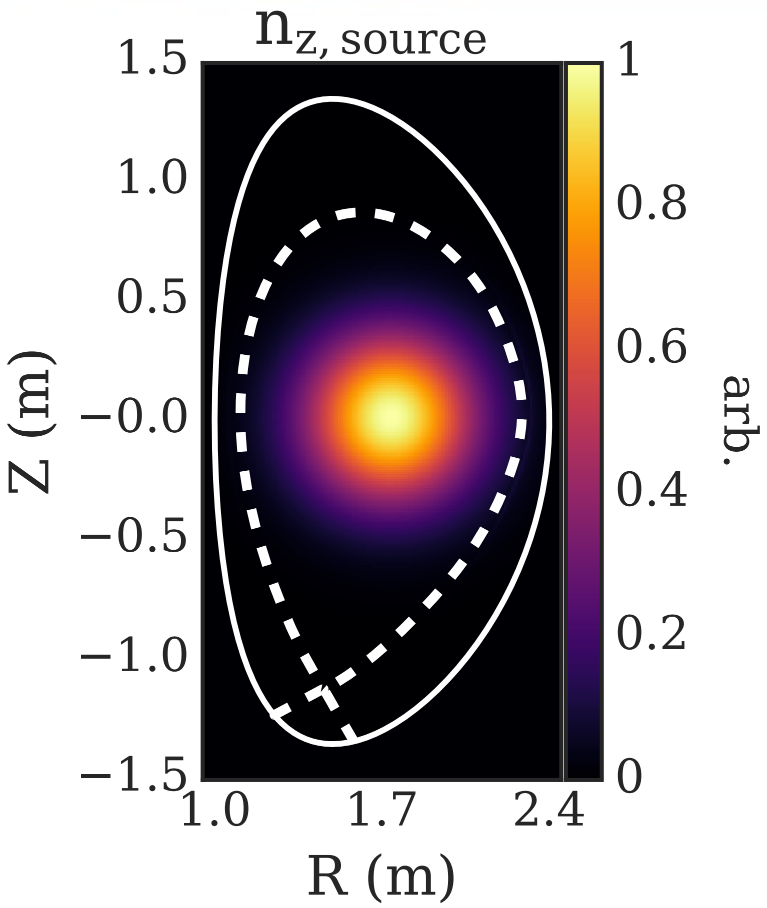

*C. R. Sovinec et al., J. Comput. Phys. 195, 355 (2004).
C. Sovinec & J. King, J. Comput. Phys. 229, 5803 (2010).

Excellent Agreement Found Between Codes in 2D

- **Quantitative agreement during thermal quench (TQ)**
- **Qualitative agreement during current quench (CQ)**
- **Low temperature in core causes resistivity to rise**
  - P_{ohm} balances P_{loss}
  - Current drops more rapidly
- **Current quench caused by contact with boundary**
- **Peak loss power when temperature on-axis falls near-zero**

Argon injection

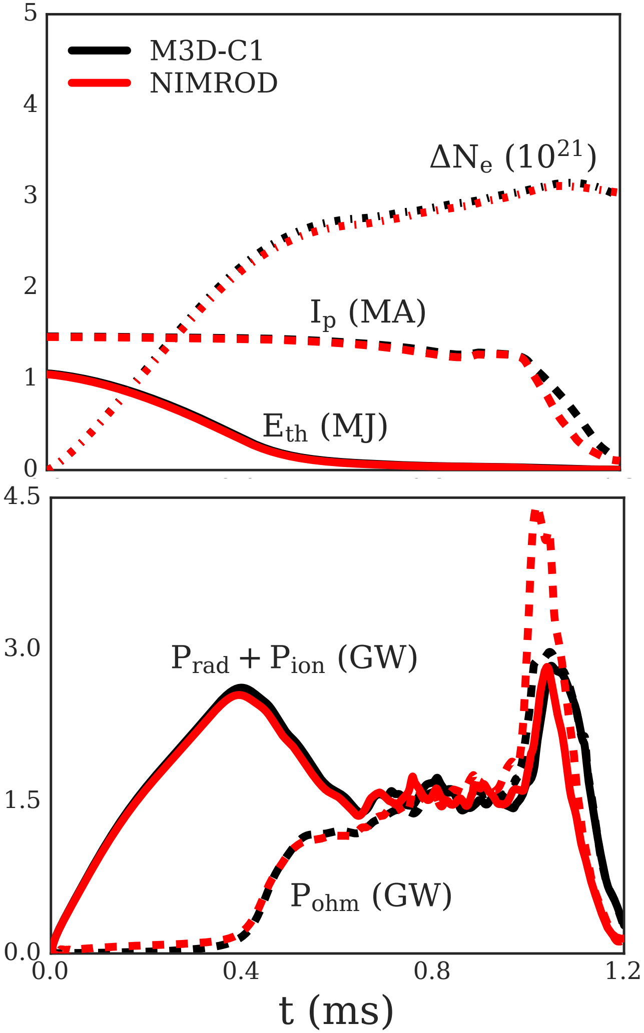

3D, Nonlinear Benchmark Between M3D-C1 & NIMROD for Realistic, Injected Pellet is Well-Underway

- **3D nonlinear MHD**
  - Fixed boundary
  - Single-temperature equation
- **Pellet/deposition parameters**
  - 3 mm radius, pure neon
  - 5 cm poloidal and 2.4 m toroidal half-width
  - 200 m/s with realistic trajectory
  - Ablation by local electron density and temperature according to model by Parks
- **Work has motivated code development and provided insight into SPI physics**

M3D-C1 Modeling of DIII-D 160606 @ 2990 ms: 0.7 MJ, 1.28 MA

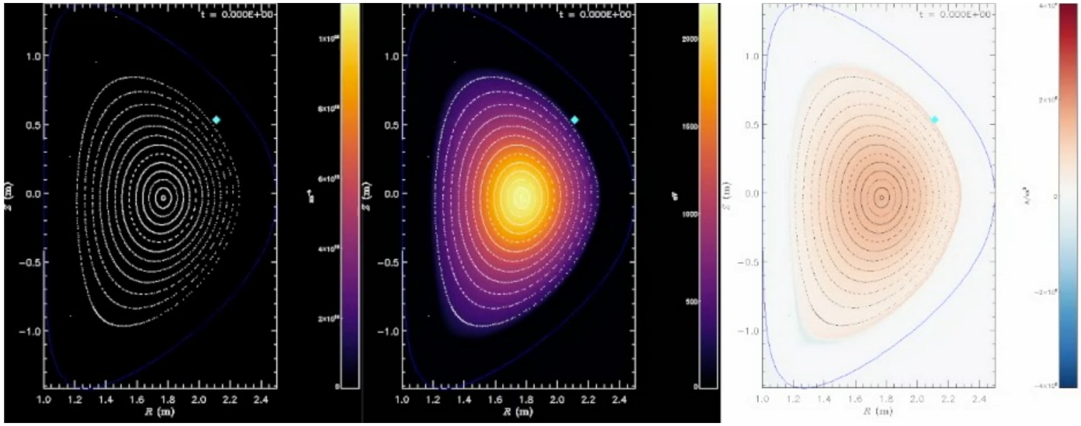
Impurity Density

Electron Temperature

Toroidal Current Density

M3D-C1 & NIMROD Differ in Timing of Instability Onset

- **Early, radiation driven thermal quench in good agreement**
- **NIMROD shows earlier spike in radiation, driven by earlier MHD instability onset**
- **M3D-C1 observes stabilization from density diffusivity**

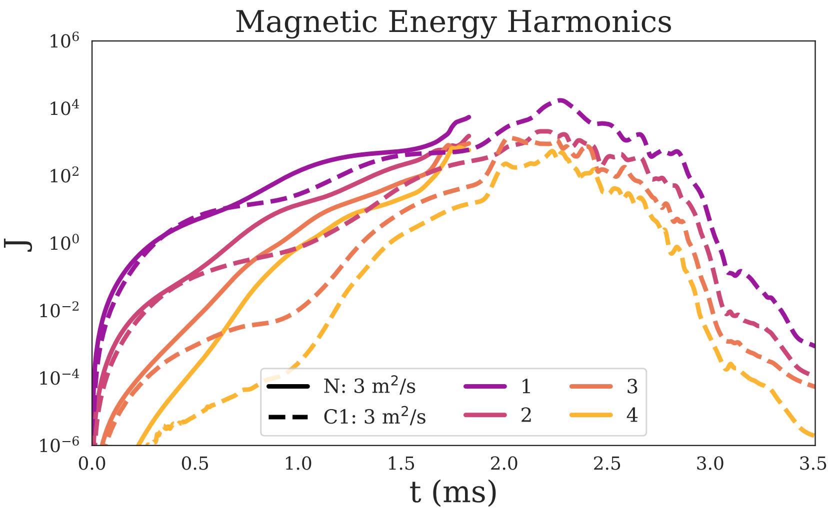

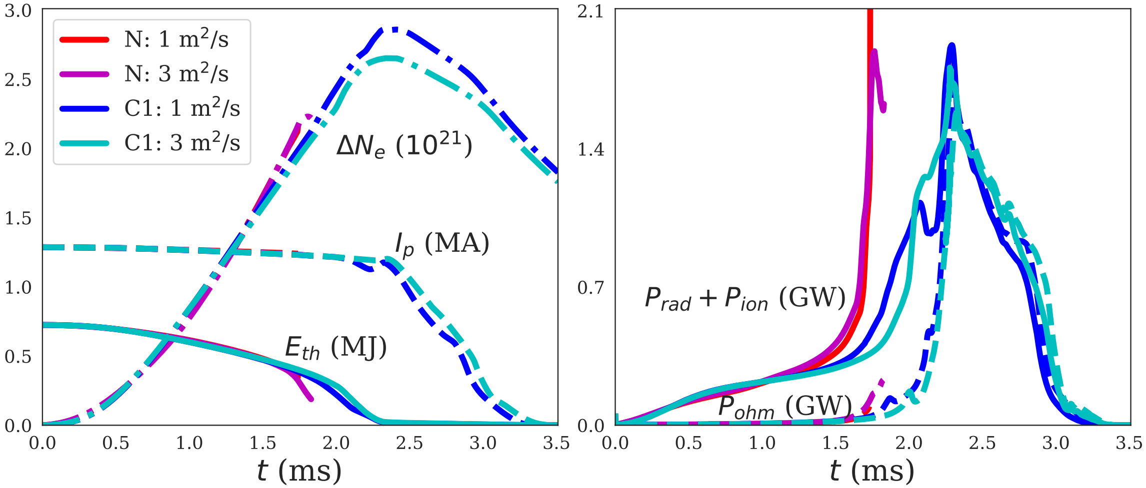

SPI Plume Modeling in JET

M3D-C1 Multi-Fragment Modeling Uses Realistic Model for Shattered Plumes

- **Script created to generate shatter plumes**
  - Uniform fragments
  - Fracture-threshold theory [T.E. Gebhart et al. IEEE 48, 6 (2019)]
- **Distribution options**
  - Sunflower distribution
  - 2D uniform
  - Gaussian poloidal/toroidal spread
- **Easily generate random (but reproduceable) plumes for different pellet size, speed, and composition**
- **Being used for reference plumes in JET & KSTAR modeling by M3D-C1, NIMROD, and JOREK**

Same parameters, different random plumes

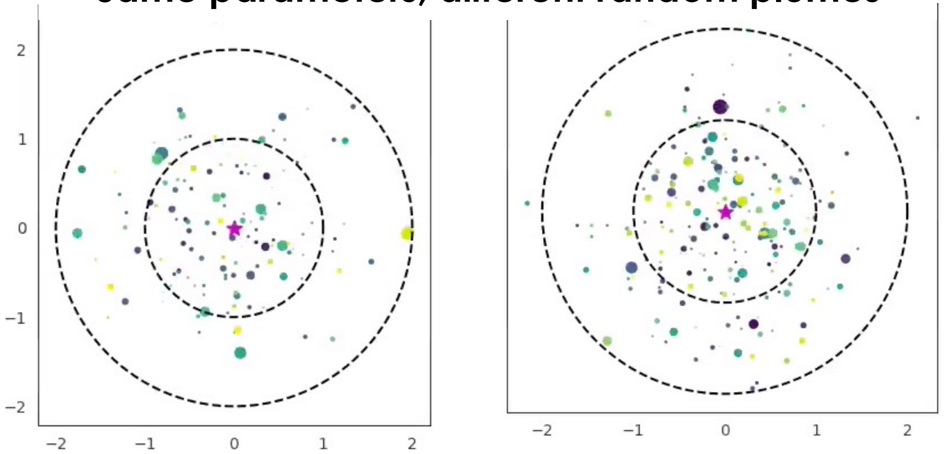

Spread in tokamak geometry

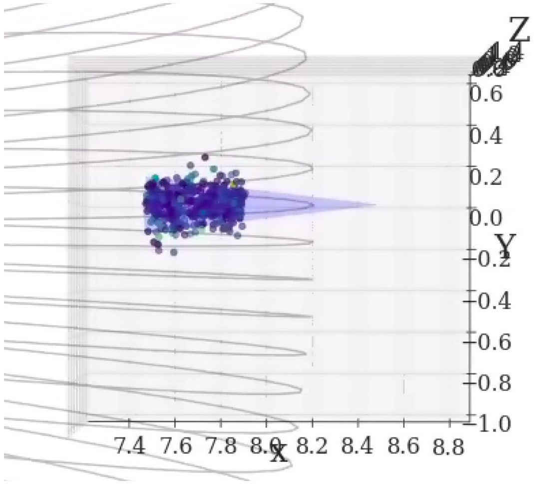

M3D-C1 JET Modeling with Realistic Plumes Performed for JET Scenario 1

- **Based on high-thermal-energy (Scenario 1) plasma with 8.1 mm cylindrical pellet**
- **Equilibria reconstructed with kinetic profiles acquired for recent experiment**
- **Two realistic pellets travel along nominal trajectory**
  - Pure Neon
    - 30 1.71-mm shards
    - 150 m/s
  - 95% D:
    - 85 1.21-mm shards
    - 300 m/s
  - Uniform shard size computed from ablation-average of cloud
- **Also consider same plumes but swapped speeds**

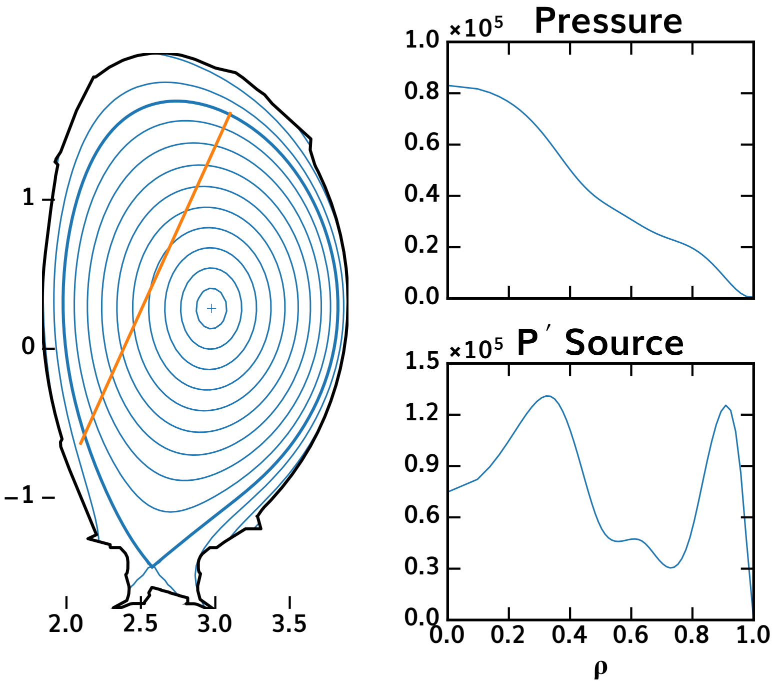

JET 95707
I_p = 2.4 MA
W_{th} = 3.4 MJ
(Scenario 1 High W_{th})

JET Modeling Shows Competition Between Rate of Travel and Rate of Radiative Dissipation

- **All plumes show similar peak radiated power**
- **Dynamics versus time**
  - Fast neon has earliest TQ
  - Others have similar TQ times
- **Dynamics versus penetration depth**
  - Slow: both travel same to same depth – *radiation dominates*
  - Fast: mixed pellet travels deeper – *doesn't radiate fast enough to induce instability*
  - Deeper penetration leads to increased mode coupling

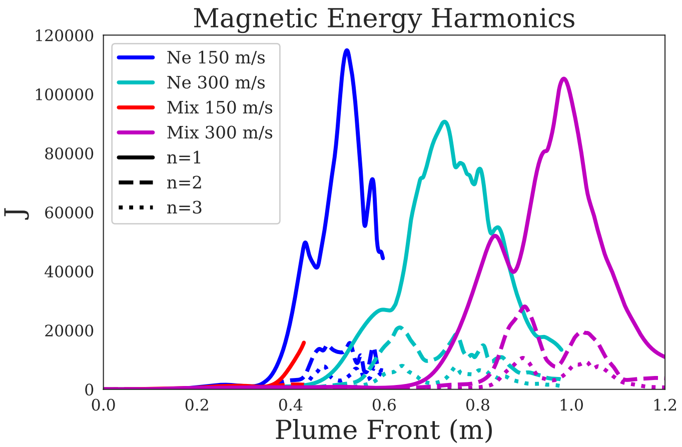

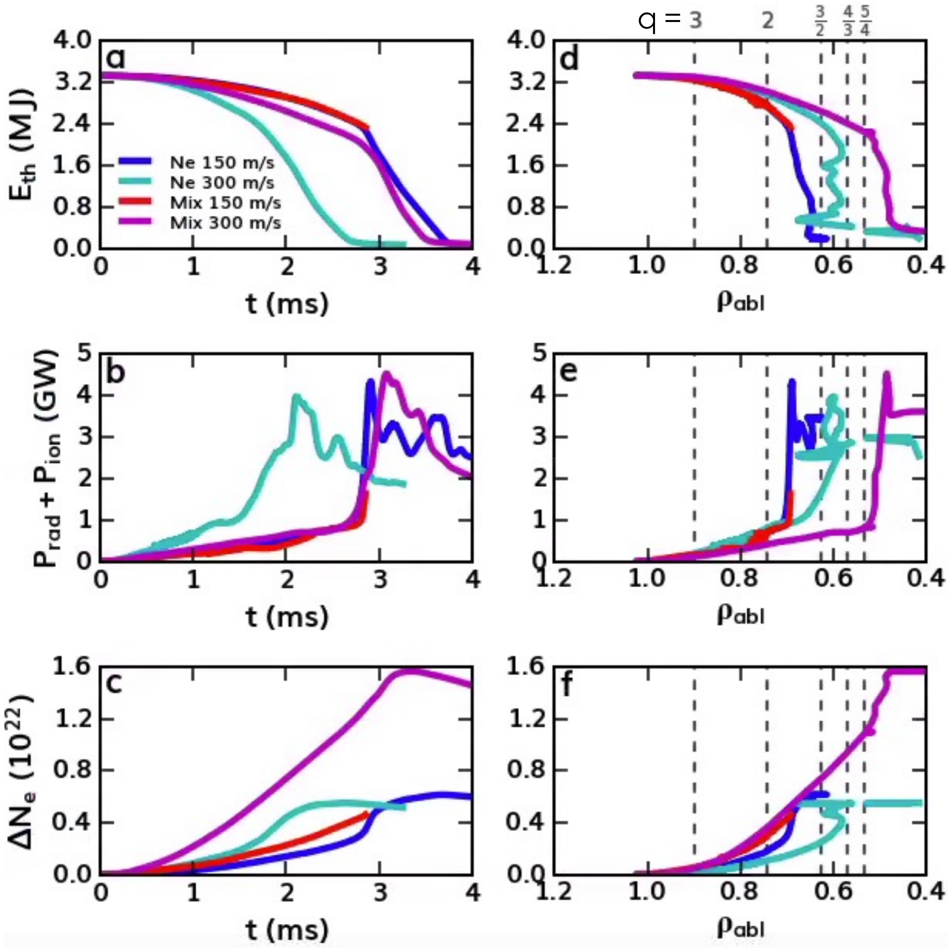

shard position, weighted by ablation rate

SPI Plume Modeling in KSTAR

Initial M3D-C1 KSTAR Modeling Shows Uncertain Benefits of Multiple Injection

- **Realistic plumes created for 7-mm, 10%-Ne pellet with 12.5˚ shatter angle**
- **Two, symmetrically injected pellets**
  - Better than **two pellets at one angle**
    - Slower TQ 👍
    - Lower peak radiation 👍
    - Lower TPF 👍
  - But not necessarily better than **one pellet**
    - Faster TQ 👎
    - Similar peak radiation, but longer duration
    - Lower TPF 👍
- **Future work**
  - 20% Ne vs. 2x 10% Ne
  - Time delays on dual injection
  - Validation with 2022 KSTAR data

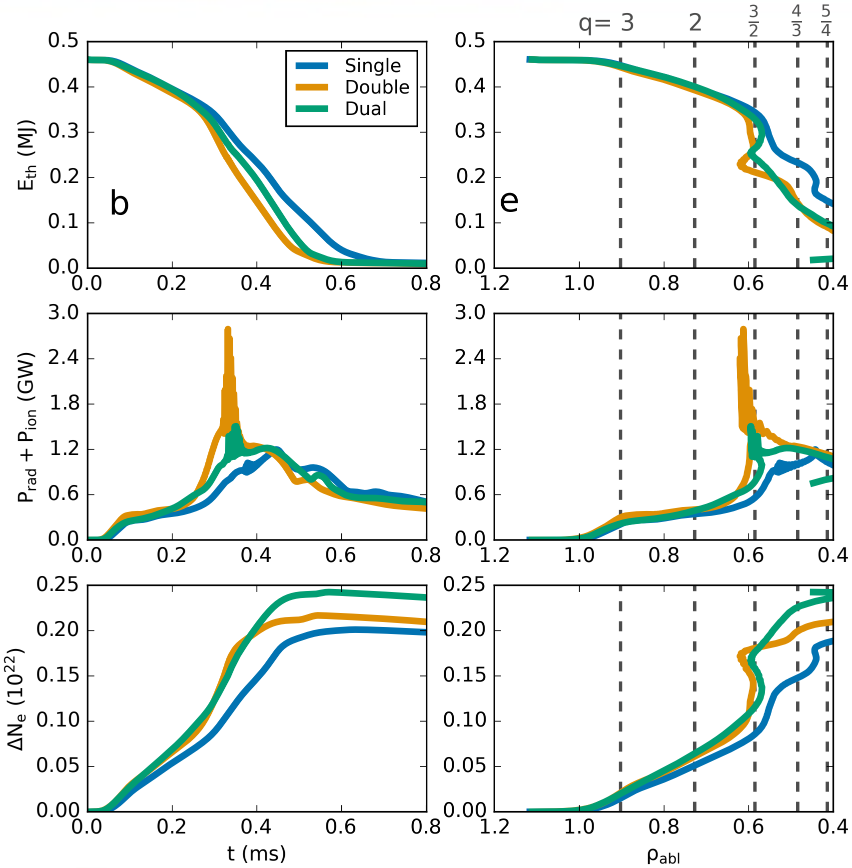

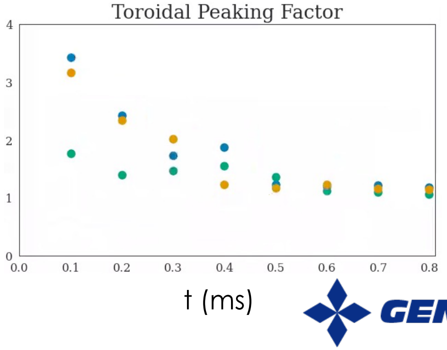

Coupling to ADAS Impurity Model

ADAS Impurity Data is Being Coupled to M3D-C1

- **Atomic Data and Analysis Structure (ADAS) provides**
  - A database of high-quality impurity data
  - Collisional-radiative data with density dependence
- **Even at low density (coronal limit), ADAS can be very different from KPRAD**

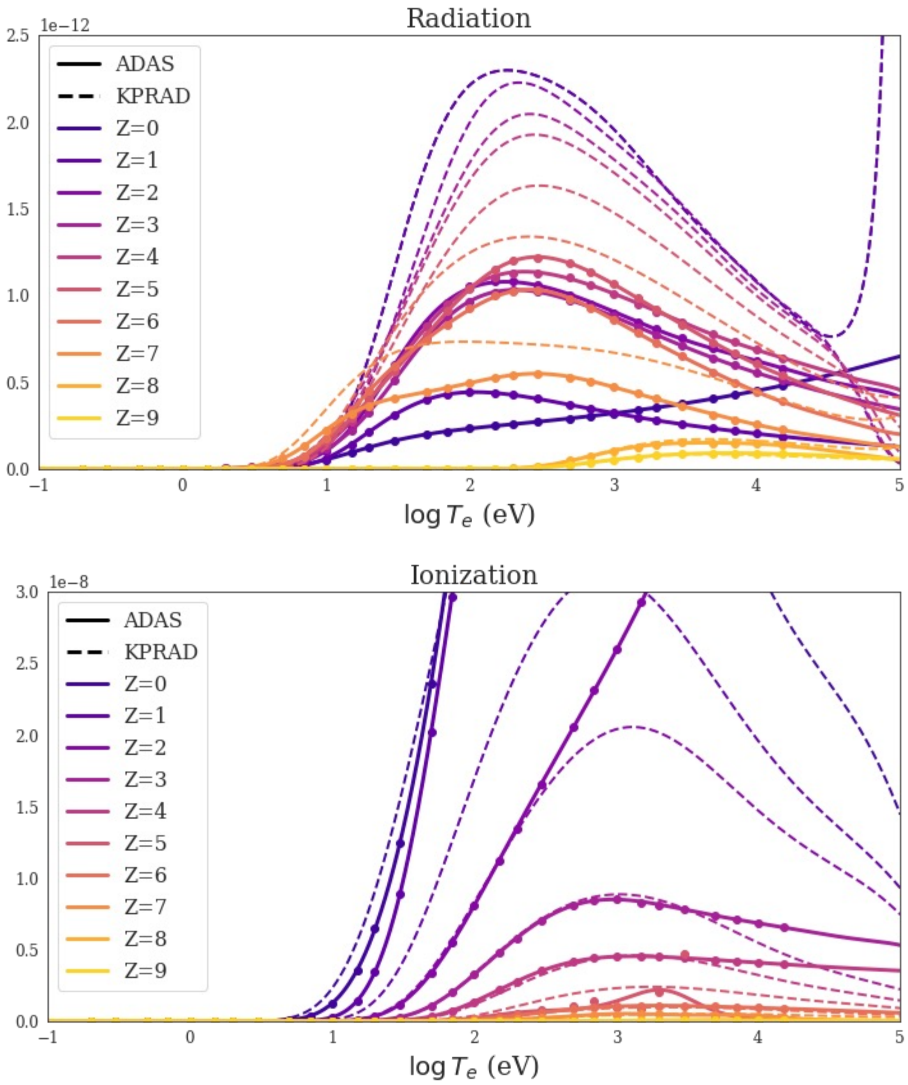

Changes in Radiation & Charge States Significantly Affect Benchmark Thermal Quench Dynamics

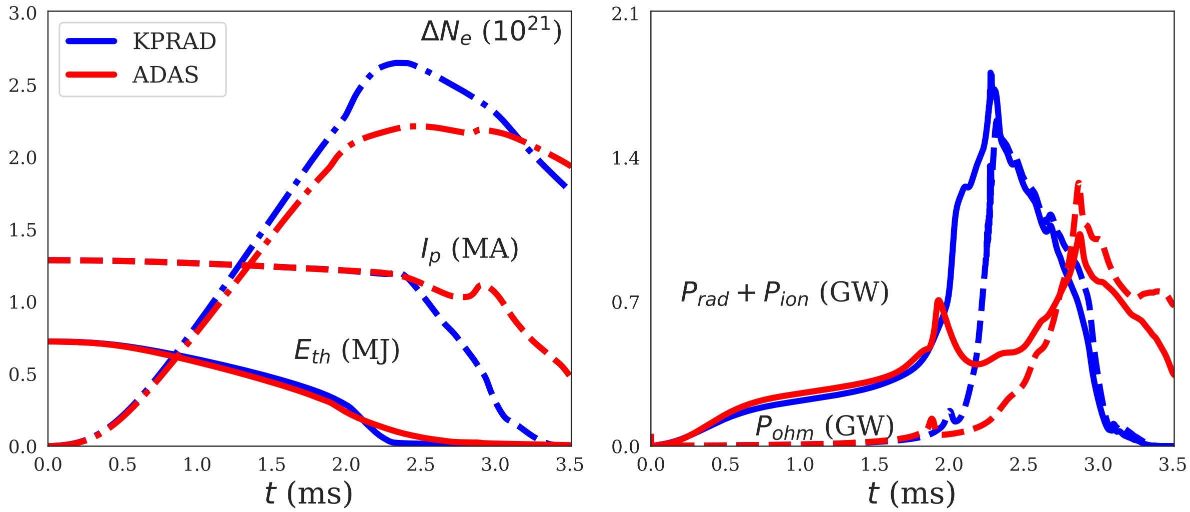

Line Radiation

KPRAD **ADAS**

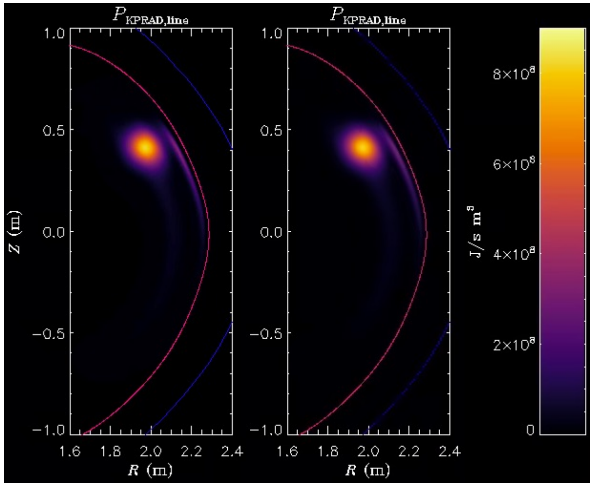

Ne 7+

KPRAD **ADAS**

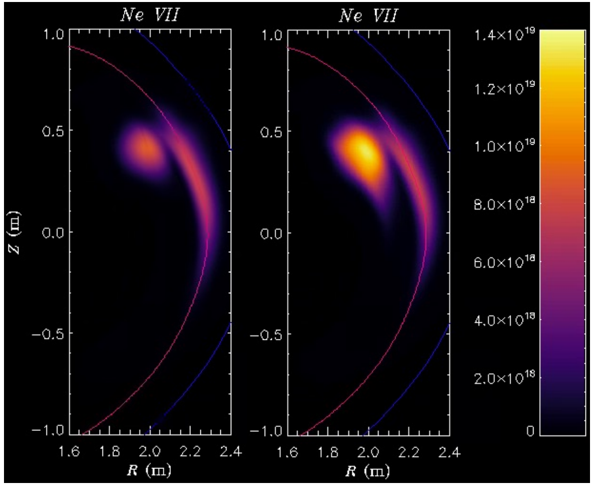

Ne 8+

KPRAD **ADAS**

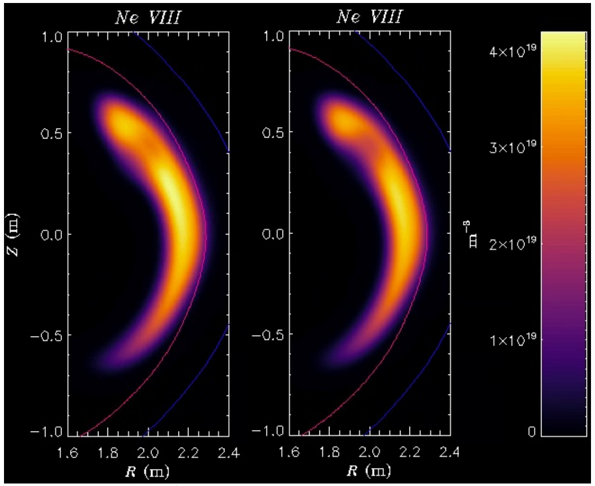

Conclusions & Future Work

- **M3D-C1/NIMROD benchmark gives confidence in 3D nonlinear MHD modeling of SPI**
- **JET simulations show competition between SPI rate of travel and rate of radiative dissipation for inducing MHD**
- **Initial KSTAR modeling shows that symmetric injection of material improves thermal quench metrics, but injecting less material overall could be better**
- **Future Work**
  - Complete benchmark
  - Simulate additional KSTAR scenarios and validate with data
  - Couple to density-dependent, collisional-radiative ADAS data

Future M3D-C1 Disruption Mitigation Work

- **M3D-C1 & NIMROD 3D benchmark**
  - Continue convergence studies
    - Poloidal & toroidal resolution
    - Time step
    - Diffusivities
  - Need to determine metrics for success
    - Strong nonlinearity makes exact agreement difficult
    - Chaotic evolution: small discrepancies early cause exponential deviation
    - Perhaps use physically relevant quantities,
      e.g., assimilation fraction, radiation fraction/peaking, TQ time
- **Validate JET modeling against experimental results**
- **Validate KSTAR modeling of multiple toroidal injection**
- **Predictive modeling for ITER SPI**

Additional Slides

Two-Temperature Modeling Shows Delayed Thermal Quench

- **M3D-C1 benchmark case re-run with two-temperature model**
- **Early dynamics similar, but deviates as electrons cool faster than single-temperature model**
  - Less ablation and ionization
  - Slower thermal quench
  - Delayed instability
- **Single-temperature model may underpredict thermal-quench times and overpredict pellet assimilation**